Supplementary Information

Materials and Methods

Plasmids

The coding sequence of the gB ectodomain (residues 22-672) (GenBank access no. BAU51603.1) was cloned from the M81 strain with residues $WY^{112-113}$ and $WLIW^{193-196}$ replaced with HSV-1 residues $HR^{177-178}$ and $RVEA^{258-261}$, respectively (1). This gB ectodomain sequence was cloned into a pCDNA3.1(+) vector with a C-terminal 6× His tag at the C-terminus and an N-terminal CD5 signal peptide for protein secretion.

The full-length complementary DNA (cDNA) sequence of NRP1 was PCR-amplified using cDNA from HK1 cells and then integrated into the pCDNA3.1(+) vector with a C-terminal 6× His tag at the C-terminus, and an N-terminal CD5 signal peptide for protein secretion.

The full-length sequences of gB and gp350 were PCR-amplified using the bacterial artificial chromosome (BAC) of EBV-M81 and then inserted into the pCDH vector. gHgL (full-length gL linked with full-length gH by a $(G_4S)_3$ linker) was also inserted into the pCDH vector.

Full-length BALF5 was PCR-amplified from EBV-M81 BAC and then inserted into the pUC19 vector. pUC19-BALF5 was used to plot the standard curve for determining the EBV DNA copies.

pCAGGS expression plasmids for gH, gL, gB, T7, and pT7EMCLuc (which carries a luciferase-containing reporter plasmid under the control of the T7 promoter) were kindly provided by Professor Richard Longnecker.

For the single alanine substitutions of gB-E345A, N348A, K349A, H352A, E353A, E356A, Q359A, D360A, R388A, L390A, R539A, K540A, S558A, T565A, K566A, T567A, H610A, F611A, K612A and T613A, the expression plasmids were directly obtained by PCR amplification using paired primers harboring each point mutation, and then the template plasmids were digested with Dpn I (Thermo Fisher Scientific) following the manufacturer's instructions before the transformation. All mutants were

also tagged with 6× His. The sequences of all plasmids were verified by Sanger sequencing.

Expression and purification of proteins and antibodies

According to the manufacturer's instructions, plasmids encoding wild-type gB (gB-WT), mutant gB, NRP1, or antibody heavy and light chains were transiently transfected into 293F cells using polyetherimide. The supernatant was collected at 5-7 days post transfection and filtered through 0.22 μm filters. The gB-WT and mutant gB were further purified with Ni^{2+} Sepharose^{TM} 6 Fast Flow beads (GE Healthcare). The target proteins were eluted by elution buffer (80 mM imidazole, 20 mM HEPES, 250 mM NaCl, pH 8.0). Purified proteins were verified by SDS-PAGE and further concentrated using a 10 kDa ultracentrifuge tube (Millipore).

The recombinant antibodies were purified from the supernatant using Protein A affinity chromatography (GE Health). The purified mAbs 3A3 and 3A5 were then labeled with horseradish peroxidase (HRP) by a periodate coupling method. The antigen-binding fragments (Fabs) of 3A3, 3A5, and AMMO5 were prepared by papain digestion (1:400 mass ratio of papain to antibody) at 37℃ for 12 hrs and further purified by a TSKgel DEAE-5PW (Tosoh Bioscience) column.

Rabbit B cell isolation and recombinant antibody cloning

Ten-week-old New Zealand White Rabbits (Songlian Laboratory Animal Center, Shanghai) were subcutaneously immunized with gB-WT mixed with an equal volume of Freund's adjuvant three times at 2-week intervals. After immunization, approximately 5 ml of blood was collected. According to the manufacturer's instructions, peripheral blood mononuclear cells (PBMCs) were isolated by Ficoll-Paque PLUS (GE Healthcare). The PBMCs were collected and washed three times with PBS. Sulfo-NHS-LC-Biotin (Thermo Fisher Scientific) conjugated gB-His was used to sort antigen-specific B cells. PBMCs (1×10^6) were suspended in 100 μL of PBS and incubated with biotin-conjugated gB-His for 30 min at 4℃. The PBMCs were washed three times with PBS and collected by centrifugation at 800 × g for 5 min.

PBMCs were labeled with a panel of reagents and antibodies for sorting: LIVE/DEAD Aqua (Thermo Fisher), mouse anti-rabbit CD4: FITC (Bio-Rad), mouse anti-rabbit CD8: FITC (Bio-Rad), mouse anti-rabbit T lymphocytes: FITC (Bio-Rad), mouse anti-rabbit IgM: RPE (Bio-Rad) and streptavidin APC conjugate (Thermo Fisher).

B cell sorting was conducted with a BD FACS Aria III cell sorter. Antigen-positive B cells were sorted into a 96-well plate containing 293T-rCD40L feeder cells expressing rabbit CD40 ligand, 20 ng/ml human interleukin 2 (Sigma-Aldrich) and 50 ng/ml human interleukin 21 (Sigma-Aldrich). B cells were cultured *in vitro* for 7 days, and the supernatant was collected for ELISA tests.

The RNA of positive B cells was extracted, and cDNA was prepared using Superscript III reverse transcriptase (Invitrogen) primed with random hexamers. Antibody variable regions of heavy and light chains were recovered via nested PCR using GXL polymerase (Takara). The primary PCR used gene-specific primers to amplify the variable region genes. The secondary PCR utilized primers containing overlapping regions of the leader sequence at the 5' end and the CH1 or Cκ region at the 3' end. The PCR product was inserted into pVRC8400 vectors containing the rabbit heavy or light chain's constant region for antibody production.

Indirect enzyme-linked immunosorbent assay (ELISA)

Indirect ELISA was performed to determine the reactivities of the purified antibodies with gB-WT and gB mutants and to monitor the serum titers of immunized rabbits. Purified gB-WT or gB mutants (100 ng/well in PBS) were coated on 96-well ELISA plates (Corning) for 2 h at 37℃. After washing with TBST, the plates were blocked with blocking buffer (PBS containing 0.5% casein, 2% gelatin, and 0.1% ProClin 300, pH 7.4) for 2 h at 37℃.

To determine antibody reactivity, 2-fold serially diluted mAbs (starting from 10 μg/ml) were added to each well and incubated for 1 h at 37℃. After washing 5 times with TBST, goat anti-rabbit antibody conjugated with HRP (Promega) diluted at a ratio of 1:5000 was added and incubated for 30 min at 37℃. To determine the human serum

titers, 3-fold serially diluted sera (starting from 1:100) were added to plates coated with gp350, gHgL, and gB (100 ng/well) and incubated for 1 h at 37℃. After washing 5 times with TBST, goat anti-human antibody conjugated with HRP (Promega) diluted at a ratio of 1:5000 was added and incubated for 30 min at 37℃.

To determine rabbit serum titer, 2-fold serial dilutions of sera (starting from 1:100) were added to the plates and incubated for 1 h at 37℃. The following steps were the same as those for the reactivity detection of antibodies. The EL-TMB kit (Sangon Biotech) was used for color development. Absorbance was measured at 450 nm and 630 nm using a microplate reader (Molecular Devices).

Competitive ELISA and antibody blocking assay

Competitive ELISA was used to detect epitope overlap of different antibodies against gB. ELISA plates (Corning) were coated with 10 ng/well gB-WT at 4℃ overnight and blocked with the above blocking buffer at 37℃ for 2 h. Primary antibodies (100 μl, 10 μg/ml) were added to the plates and then incubated at 37℃ for 30 min. After washing five times, HRP-conjugated secondary antibodies were added and incubated at 37℃ for 30 min. TMB substrates were added, and the absorbance was measured at 450 nm and 630 nm using a microplate reader (Molecular Devices). All samples were tested three times. The competitive ability of primary antibodies against secondary antibodies was calculated using the following equation: Percentage of competition% = [OD(-Primary/+Secondary) - OD(+Primary/+Secondary)]/OD(-Primary/+Secondary) ×100%.

Competitive ELISA was also used to detect 3A3- and 3A5-like antibodies in human sera. gB (100 ng/well) was coated in a 96-well plate. In a serially diluted pre-test ELISA, the dilution folds of human sera to produce 1 OD reading value were determined. In the blocking assays, 100 μl of mAbs 3A3, 3A5, 3A3+3A5, 1E12 or 2G9 (10 μg/well) was added and incubated at 37℃ for 30 min. After five washes, the predetermined dilution of human sera with 1 OD reading was added for another 30 min. After five washes, goat anti-human IgG antibody conjugated with HRP (Promega) was added and incubated at

37℃ for 30 min. The color was developed as in the indirect ELISA. The blocking ratio of the mAb against each serum sample (dots) was calculated as 1- (OD value of the sera binding to coated antigens treated with mAb/OD value of the sera binding to coated antigens without mAb treatment) × 100%.

Antibody blocking assay by flow cytometry

1×10^5 293T-gB cells were washed with 0.5% BSA in PBS three times and then incubated with 10 μg 3A3, 3A5, 3A3+3A5, 1E12, 2G9 or 50 μl 0.5% BSA in PBS at 37ºC for 30 min, respectively. After washing with 0.5% BSA in PBS three times, the cells were incubated with 50 μl 1:500 diluted human sera from 15 healthy donors and 15 patients with NPC at 37ºC for 30 min. Then the cells were washed three times with 0.5% BSA in PBS and stained with goat anti-rabbit IgG AlexaFluor 488 (1:500, Invitrogen) antibody and goat anti-human IgG AlexaFluor 647 (1:500, Invitrogen) antibody at 4ºC for 30 min. After being washed with 0.5% BSA in PBS three times, data were collected with CytoFLEX (Beckman Coulter) and analyzed using FlowJo software X 10.0.7 (Tree Star). Cells that were not incubated with mAbs or human sera were used as a negative control. Cells incubated without mAbs and only with human sera were used as positive controls for each blocking assay. The blocking ratio of the mAb against each serum was calculated as 1- (AF647 positive cells incubated with mAbs/AF647 positive cells incubated without mAbs) × 100%.

Immunofluorescence assay

Cells overexpressing gB, gHgL, gp350, or vector were seeded on glass coverslips in 12-well plates for 24 h. Cells were washed twice with PBS and fixed for 10 min with 4% paraformaldehyde at room temperature. Following fixation, the cells were incubated in blocking solution (5% BSA, 0.5% Triton X-100 in PBS) for 1 h at room temperature and incubated overnight at 4ºC with primary antibodies. After being washed with PBS three times, the cells were incubated with secondary antibodies. Cells incubated without primary antibodies were used as a negative control. Images were captured with an FV1000 OLYMPUS microscope.

3A3 (1:200), 3A5 (1:200), AMMO5 (1:200), anti-Flag (1:200), 72A1 (1:200) or AMMO1 (1:200) was used as primary antibodies. Goat anti-rabbit IgG AlexaFluor 488 (1:1000, Invitrogen), goat anti-mouse IgG AlexaFluor 488 (1:1000, Invitrogen), goat anti-human IgG AlexaFluor 488 (1:1000, Invitrogen), goat anti-rabbit IgG AlexaFluor 647 (1:1000, Invitrogen), goat anti-mouse IgG AlexaFluor 647 (1:1000, Invitrogen) or goat anti-human IgG AlexaFluor 647 (1:1000, Invitrogen) was used as secondary antibodies.

Antibody depletion from human sera

Human sera from 45 healthy adult donors (15 sera for the antibody depletion assay and 30 sera for antibody blocking assay) and 30 NPC patients (30 sera for antibody blocking assay) were collected from Sun Yat-sen University Cancer Center. All sera were treated at 56°C for 45 min to inactivate the complement, and no extra complement was added. The titers of serum antibodies against EBV antigens were also measured using commercial kits from Euroimmun (Lübeck, Germany) for VCA-IgM and VCA-IgG and IBL (Hamburg, Germany) for VCA-IgA, EA-IgA, EA-IgG, EBNA-1-IgA, and EBNA-1-IgG according to the manufacturers' instructions. Briefly, the levels of seromarkers were standardized by calculating the ratio of the optical density (OD) of the sample to that of a reference control (rOD). The positive cutoff values for the rOD were indicated by the manufacturer's instructions. A nasopharyngeal carcinoma patient is expected to be positive for VCA-IgG, VCA-IgA, EA-IgA, and EBNA-1-IgA. An asymptomatic EBV carrier is expected to be positive for VCA-IgG and EBNA-1-IgG but negative for VCA-IgA, EBNA-1-IgA, VCA-IgM and EA-IgG (2-4).

3×10^6 293T cells that stably expressed gp350, gB, or gHgL were collected into individual tubes and washed with PBS twice. Then, 100 μl human serum samples were added to each tube's 293T cell pellet. After thorough pipetting to mix sera and 293T cells, the mixture was incubated on ice for 1 h to deplete the gp350, gB, or gHgL-specific antibodies. The human serum supernatant was transferred to another tube of antigen-expressing 293T cells after centrifugation at 200 × g. Before and after 15 rounds of depletion, the total gp350, gB, and gHgL-specific IgG antibodies in each serum were

determined by indirect ELISA. 293T cells stably transfected with the empty vector were used as the negative control in this depletion assay. The IgG titers were calculated by the endpoint dilution method, and the OD450=0.1 was set as the cut-off value. The percentage of IgG titer reduction was calculated by the formula (1-IgG $titer_{-depleted}$/IgG $titer_{-before}$) × 100%, where IgG $titer_{-depleted}$ is each glycoprotein-specific IgG titer of the serum after the specific antibody depletion, and IgG $titer_{-before}$ is each glycoprotein-specific serum IgG titer before depletion.

Binding to induced Akata-EBV-GFP cells

The EBV-positive Akata cells were induced at 37℃ by goat anti-human IgG (0.8% v/v) in RPMI 1640 without FBS at a cell density of 2×10^6 cells/ml for 6 hrs and subsequently cultured in fresh RPMI 1640 with 10% FBS for 48 hrs. Then, the cells were washed with PBS and collected for the binding assay. Single-cell suspensions were incubated with anti-human FcR block (BioLegend) for 30 min at 4℃, fixed and permeabilized with Fixation Buffer/Permeabilization Wash Buffer (BioLegend) and stained with 3A3 (1:200), 3A5 (1:200), AMMO5 (1:200) and anti-Flag (1:200) for 30 min at room temperature. After being washed three times with PBS, cells were incubated with goat anti-rabbit IgG Alexa Fluor 488 (1:1000, Invitrogen), goat anti-mouse IgG Alexa Fluor 488 (1:1000, Invitrogen), and goat anti-human IgG Alexa Fluor 488 (1:1000, Invitrogen) secondary antibodies. Cells incubated without primary antibodies were used as the negative control. Data were collected with CytoFLEX (Beckman Coulter) and analyzed using FlowJo software X 10.0.7 (Tree Star).

Cryo-EM sample preparation and data collection

Complexes of gB:3A3Fab, gB:3A5Fab and gB:3A3Fab:3A5Fab (molar ratios of 1:4, 1:4 and 1:4:4) were prepared respectively and purified by TSK-Gel 3000PWxl (TOSOH) and then concentrated to 2 mg/ml. Aliquots (3 μl) of purified immune complexes were deposited onto fresh glow-discharged holey carbon Quantifoil Cu grids (R1.2/1.3, 200 meshes, Quantifoil Micro Tools). Grids were blotted for 6 s at 100% humidity and 4℃ for plunge-freezing (Vitrobot Mark IV, FEI) in liquid ethane cooled

by liquid nitrogen. Cryo-EM datasets of gB:3A3Fab and gB:3A5Fab were recorded on a FEI Tecnai F30 TEM equipped with a Falcon3 direct electron detector at a nominal magnification of 93,000 ×, corresponding to a pixel size of 1.12 Å. 771 and 734 movies were collected for gB:3A3Fab and gB:3A5Fab complexes, respectively. The dataset of gB:3A3Fab:3A5Fab was recorded on a FEI Titan Krios equipped with a Gatan imaging filter (GIF) and a post-GIF Gatan K2 Summit direct electron detector at a nominal magnification of 21,000 ×, corresponding to a pixel size of 1.1 Å. 4,779 movies were collected for gB:3A3Fab:3A5Fab complex. The total electron dose of each movie was approximately 60 e-/Å2, which was fractionated into 39 frames (Falcon3) or 40 frames (K2-summit) with an exposure time of 1 s (Falcon3) or 8 s (K2-summit), respectively. Data were automatically collected using FEI EPU on F30 TEM and SerialEM software(5) on Titan Krios TEM.

Image processing and three-dimensional reconstruction

Frames of each movie were aligned and motion corrected using MotionCor2 (6), and the contrast transfer function parameters of micrographs were determined with Gctf (7). Micrographs with excessive drift or astigmatism were discarded before reconstruction. Particles were automatically picked and screened using Gautomatch (https://www2.mrc-lmb.cam.ac.uk/research/locally-developed-software/zhang-software/#gauto) or cryoSPARC 2.4.2 (8). The initial 3D models of each dataset were generated with a random model method using cryoSPARC 2.4.2. To select good particles for further refinement, multiple rounds of reference-free two-dimensional (2D) classification were performed using cryoSPARC 2.4.2 or Relion 2.1 (9). For gB:3A3Fab and gB:3A5Fab, 9,270 and 18,826 2D particles were subjected to final homogenous refinement using cryoSPARC 2.4.2 to obtain the moderate resolution density maps of two immune-complexes. For gB:3A3Fab:3A5Fab complex, 3D classification was performed with 463,280 particles using Relion 2.1, and 367,966 good classes were then selected for further refinement and post-processing by software cisTEM (10). The final resolutions of all reconstructions were evaluated using the gold-standard Fourier shell correlation (threshold = 0.143 criterion) (11). The local resolution was evaluated by

ResMap (12).

Model building and refinement

The X-ray crystal structure of gB (PDB code: 3FVC), which served as a homology model, was fitted into the segmented volume of the final cryo-EM density map of gB:3A3Fab:3A5Fab using UCSF Chimera (13) and rebuilt with Coot (14). For 3A3Fab and 3A5Fab, the initial atomic models for the variable domains of Fabs were generated by homology modeling using Accelrys Discovery Studio software (https://www.3dsbiovia.com/products/collaborative-science/biovia-discovery-studio/). The models were further improved using phenix.real_space_refine in PHENIX (15). The model statistics, including bond lengths, bond angles, all-atom clashes, rotamer statistics, and Ramachandran plot statistics, were closely inspected with Coot throughout the process. The final atomic models were validated using MolProbity (16). Model statistics are summarized in Table S2. The buried area of the interaction interface between each Fab and one protomer of gB trimer was analyzed using the PISA server (https://www.ebi.ac.uk/pdbe/pisa/) and the CCP4 program suite (17) with donor-to-acceptor distances ≤4 Å for hydrogen bonding interactions. All figures were generated with UCSF Chimera or PyMOL (https://pymol.org/2/).

Virus production

Akata-EBV-GFP cells were resuspended in RPMI 1640 to a density of 2×10^6 cells/ml. Goat anti-human IgG (Tianfun Xinqu Zhenglong Biochem.Lab) was added to the cell suspension at a concentration of 0.8% (v/v) to induce EBV production for 6 h. CNE2-EBV-GFP cells were induced by 12-O-tetradecanoylphorbol 13-acetate (TPA) (20 ng/ml) and sodium butyrate (2.5 mM) for 12 h. After culture in fresh RPMI 1640 with 10% FBS for 72 h, the supernatant was filtered through 0.45 μm filters to collect the virus. The EBV virus was further concentrated 100-fold by centrifugation at 50,000 × g for 2.5 h and resuspended in fresh RPMI 1640 without FBS. The EBV virus was stored at -80℃ and thawed immediately before use.

For lentivirus production, 293T cells were transfected with psPAX2, pMD2.G and

pCDH-gB-flag-puro/pCDH-gp350-flag-puro/pCDH-gLgH-flag-puro at a mass ratio of 3:2:5 using PEI. The supernatant was collected 48 h after transfection, filtered through 0.45 μm filters and then mixed with 5 × PEG8000 NaCl solution at 4℃ overnight. Lentivirus was collected by centrifugation at 4,000 × g at 4℃ for 1 h and resuspended in RPMI 1640. The lentivirus was stored at -80℃ and thawed immediately before use.

Neutralization assays

All sera used in this assay were treated at 56℃ for 45 min to inactivate the complement, and no extra complement was added. For B cell neutralization, 2-fold serially diluted antibodies (starting from 100 μg/ml) or 2-fold serially diluted human sera (starting from 1:10 dilution) were incubated with 20 μl (2,000 green Raji units (GRUs)) of CNE2-EBV-GFP for 2 h at 37°C. Subsequently, the mixtures were added to 1×10^4 EBV-negative Akata B cells in 96-well plates and incubated for 3 h at 37°C. For epithelial cell neutralization, 2-fold serially diluted purified antibodies (starting from 100 μg/ml) were mixed and incubated with 50 μl (2,500 GRUs) Akata-EBV-GFP for 2 h at room temperature. The mixture was added to 5×10^3 HNE1 epithelial cells/well in 96-well plates and then incubated for 3 h at 37°C.

Then, the free EBV viruses in the culture medium in both assays were removed by washing with PBS once. After the cells were further cultured in fresh RPMI 1640 with 10% FBS for 48 h and washed once with PBS, the infection rate was determined by detecting and analyzing the numbers of GFP-positive cells using CytoFLEX (Beckman Coulter) and FlowJo software X 10.0.7 (Tree Star). EBV-negative Akata B cells and HNE1 epithelial cells were used as negative controls in the B cell and epithelial cell neutralization assays, respectively. EBV-negative Akata B cells and HNE1 epithelial cells incubated with EBV without antibodies were used as positive controls in the B cell and epithelial cell neutralization assay.

The neutralizing efficiency of antibodies was calculated using the following formula: neutralization % = 1- the percent of infected cells with serum or mAb/the percent of infected cells without serum or mAb × 100%. The inhibition profiles were fitted to a sigmoid trend to generate the IC_{50} value.

The reduction in the neutralizing titer of the human serum after the depletion of gp350-, gB- or gHgL-specific serum antibodies was calculated by the formula $(1\text{-}IC_{50\text{-depleted}}/IC_{50\text{-before}}) \times 100\%$, where $IC_{50\text{-depleted}}$ is the neutralizing titer of the serum depleted by specific glycoprotein-expressed 293T cells, and $IC_{50\text{-before}}$ is the neutralizing titer of the serum before depletion.

Surface plasmon resonance (SPR)

SPR-based antibody affinity (KD value) was determined using Biacore 8000 (Cytiva). The sensor chip NTA was used to immobilize gB protein by metal chelation. 0.5 mM of $NiCl_2$ was loaded for ligand capture. EBV gB was loaded at a 2 μg/ml concentration for 60 s. The serially diluted 3A3, 3A5, or AMMO5 Fabs were injected at 30 μL/min for 200 s (association phase) and then dissociated at 30 μL/min for 400 s (dissociation phase). The chip was regenerated by one injection of 350 mM EDTA after each run. The results were analyzed by BIAcore Insight Evaluation software (Cytiva). The curve fitting was performed using a 1:1 interaction model and χ^2 values less than 10% of the R_{max} value were acceptable.

Analytical ultracentrifugation (AUC)

Sedimentation velocity was used to monitor the binding of the antigen and mAb in PBS. The experiments were conducted at 20℃ on a Beckman XL-A analytical ultracentrifuge equipped with absorbance optics and an An60-Ti rotor (Beckman Coulter). All samples were diluted to ~ 1 OD at 280 nm in PBS buffer in a 1.2 cm light path. The speed was set to 36,000 rpm for gB-WT or gB mutants, 38,000 rpm for 3A3 Fab or 3A5 Fab, and 30,000 rpm for immune complexes. gB-WT or its mutants and 3A3 Fab or 3A5 Fab were mixed at a molar ratio of 1:5 and incubated for 1 h at 37 ℃ to generate immune complexes. The sedimentation coefficient was obtained using the c(s) method with Sedfit software.

Virus-free epithelial cell fusion assay

HEK-293T cells were seeded in 10 cm dishes in DMEM with 10% FBS at a density

of 2×10^6 cells/dish. Upon reaching 80% confluence, effector HEK-293T cells were transfected with 2.5 μg each of pCAGGS-gB or pCAGGS-gB-mutants, pCAGGS-gH, pCAGGS-gL, and pCAGT7 polymerase that expresses T7 DNA polymerase, while recipient HEK-293T cells were transfected with 10 μg of pT7EMCLuc, which expresses the luciferase reporter gene under the control of the T7 promoter. Twenty-four hours after transfection, 2×10^5 effector cells were trypsinized and incubated with 20 μg of 3A3, 3A5, 3A3+3A5, and 1E12 at 37℃ for 30 min. Then, the target cells were mixed and co-cultured with 2×10^5 recipient cells in a 24-well plate for another 24 h at 37℃ in DMEM with 10% FBS. The cocultured cells were lysed and luciferase activity was quantified using a Dual-Glo luciferase assay following the manufacturer's instructions (Promega).

Quantification of the cell surface and total expression of gB mutants

HEK-293T cells were seeded in 10 cm dishes in DMEM with 10% FBS at a density of 2×10^6 cells/dish. Upon reaching 80% confluence, the cells were transfected with 2.5 μg of gB mutants, including H352A, E356A, D360A, H540A, T567A, H610A, T613A, and gB-WT. Cells were collected at 24 h after transfection and incubated with 100 μg/ml 3A3 or 3A5 at 4℃ for 30 min. After washing with PBS, a 1:500 diluted goat anti-rabbit IgG Alexa Fluor 647 antibody (Invitrogen) was added and incubated at 4℃ for 30 min to detect cell surface expression. Total expression of gB mutants was determined using the same protocol, except that cells were permeabilized according to the eBioscience™ Intracellular Fixation & Permeabilization Buffer Set (Invitrogen) kit before adding the primary antibodies. The assay was performed using CytoFLEX (Beckman Coulter), and AF647 positive cells were analyzed using FlowJo software X 10.0.7 (Tree Star).

Cell surface binding assay

gB or BSA (Sigma) was labeled with AF488 NHS Ester (Lumiprobe) at a molar ratio of 1:8 (gB: AF488 NHS Ester). NRP1 was biotinylated at a 1:1 ratio (biotin: NRP1) using a biotinylation kit (Genemore) according to the manufacturer's instructions.

Biotinylated proteins were conjugated with streptavidin-phycoerythrin (SA-PE; eBioscience) at a 4:1 ratio of biotin to streptavidin.

BSA-AF488 or gB-AF488 (2.5 μg) was mixed with 35 μg of 3A3, 3A5, AMMO5, or 1E12 in 50 μl of PBS. The mixtures were added to individual 96-well plates and then incubated at room temperature for 1.5 h. AGS and HK1 epithelial cells were trypsinized, washed with PBS, and incubated in a complete medium at 37℃ for 30 min for a recovery. Then, recovered AGS and HK1 epithelial cells, and Akata and Raji B cells were centrifuged at 450 × g for 5 min and resuspended in ice-cold 0.5% BSA (Sigma) in PBS. Then, 100 μl of 1×10^5 cell suspension was mixed with BSA-AF488 and gB-AF488 with/without antibodies and incubated on ice for 1 h. Cells were collected by centrifugation at 450 × g for 5 min, washed with 0.5% BSA, resuspended and fixed in 4% paraformaldehyde. The assay was performed using CytoFLEX (Beckman Coulter), and AF647-positive cells were analyzed using FlowJo software X 10.0.7 (Tree Star).

Twenty-four hours after transfection with gB-WT or gB mutants, 293T cells were trypsinized, washed with PBS, and incubated in a complete medium at 37℃ for 30 min. 3A3 (35 μg) was mixed with 1×10^5 cells and then incubated at 37℃ for 1.5 h. SA-PE-NRP1 or SA-PE (2.5 μg) in 50 μl of PBS was added to each well and incubated on ice for 1 h. The following steps were the same as described above.

EBV infection in humanized mice

All animal experiments were performed under protocols approved by the Sun Yat-sen University Cancer Center Animal Care and Use Committee. Humanized mice were established by an i.v. injection of human cord blood $CD34^+$ hematopoietic stem cells into 4-week-old NOD.Cg-*Prkdc*^{em1IDMO}*Il2rg*^{em2IDMO} (NOD-*Prkdc*^{null} *IL2Rγ*^{null}, NPI®) mice (BEIJING IDMO Co., Ltd) 48 hrs post a single dose of Busulfan via i.p. injection at 20 mg/kg body weight. Each mouse was i.p. injected with 400 μg (~20 mg/kg) experimental or control antibodies 8 weeks post $CD34^+$ stem cell transfer. After 24 h, all the mice received a dose of Akata-EBV-GFP (25,000 GRUs) via i.v. injection. In the following four weeks, the mice received a dose of 400

μg/mouse (~20 mg/kg) of antibodies weekly. Blood samples were collected, and bodyweights were recorded weekly. The mice were euthanized at the 8th-week post-challenge or earlier if the mice had a bodyweight loss ≥ 20%.

Detection of EBV DNA in blood and tissues

DNA was extracted from the peripheral blood (50 μl) or tissues of mice using commercial DNA extraction kits (Omega). Then EBV copy numbers were detected by real-time polymerase chain reaction (RT-PCR) using primers (F: 5'-GGTCACAATCTCCACGCTGA-3'; R: 5'-CAACGAGGCTGACCTGATCC-3') to amplify a fragment of BALF5. The copy numbers of EBV were quantified using a standard curve plotted with a serially diluted plasmid of pUC19-BALF5.

H&E staining, IHC, and in situ hybridization

Tissue samples were fixed in 10% formalin and embedded in paraffin. The treated samples were stained with hematoxylin and eosin (H&E). EBERs were detected by in situ hybridizations using an EBER detection kit (ZSGB-BIO) according to the manufacturer's instructions. Immunostaining of human B cells was performed using an hCD20 antibody (Abcam) at a 1:200 dilution.

Flow cytometry assay of human cells in humanized mice

The peripheral blood of mice was treated with 1 ml of red blood cell lysis buffer (BioLegend) at room temperature for 10 min. Then, the cells were centrifuged at 300 × g, washed twice with PBS, resuspended in PBS, and stained with antibodies including anti-human CD45-APC/Cy7, CD19-APC, CD3-FITC, CD4-pacific blue, CD8-PC5.5, CD69-PC7, CD137-APC, CD38-BV650, CD24-PC5.5 and anti-mouse CD45-BV510 (Biolegend) for 30 min at 4°C. The assays were performed with a CytoFLEX (Beckman Coulter), and the data were analyzed using FlowJo software X 10.0.7 (Tree Star).

Rabbit immunization

New Zealand white rabbits (n=3) were immunized subcutaneously (s.c.) with soluble gB at a dose of 500 μg three times at 2-week intervals. Blood samples were collected two weeks after the third injection, and the serum titers of anti-gB antibodies were detected by ELISA. PBMCs were collected for B cell sorting.

Statistical analysis

All statistical analyses were conducted with GraphPad Prism version 8. Statistical tests, n and *P* values are indicated in figure legends.

References

1. M. Backovic, R. Longnecker, T. S. Jardetzky, Structure of a trimeric variant of the Epstein-Barr virus glycoprotein B. *Proceedings of the National Academy of Sciences of the United States of America* **106**, 2880-2885 (2009).
2. H. Chen *et al.*, Evaluation of a semi-quantitative ELISA for IgA antibody against Epstein-Barr virus capsid antigen in the serological diagnosis of nasopharyngeal carcinoma. *International journal of infectious diseases : IJID : official publication of the International Society for Infectious Diseases* **25**, 110-115 (2014).
3. R. Gao *et al.*, Evaluation of seven recombinant VCA-IgA ELISA kits for the diagnosis of nasopharyngeal carcinoma in China: a case-control trial. *BMJ open* **7**, e013211 (2017).
4. N. Obel, M. Hoier-Madsen, H. Kangro, Serological and clinical findings in patients with serological evidence of reactivated Epstein-Barr virus infection. *APMIS* **104**, 424-428 (1996).
5. D. N. Mastronarde, Automated electron microscope tomography using robust prediction of specimen movements. *J Struct Biol* **152**, 36-51 (2005).
6. S. Q. Zheng *et al.*, MotionCor2: anisotropic correction of beam-induced motion for improved cryo-electron microscopy. *Nature methods* **14**, 331 (2017).
7. K. Zhang, Gctf: Real-time CTF determination and correction. *Journal of structural biology* **193**, 1-12 (2016).
8. A. Punjani, J. L. Rubinstein, D. J. Fleet, M. A. Brubaker, cryoSPARC: algorithms for rapid unsupervised cryo-EM structure determination. *Nat Methods* **14**, 290-296 (2017).
9. D. Kimanius, B. O. Forsberg, S. H. Scheres, E. Lindahl, Accelerated cryo-EM structure determination with parallelisation using GPUs in RELION-2. *Elife* **5**, e18722 (2016).
10. T. Grant, A. Rohou, N. Grigorieff, cisTEM, user-friendly software for single-particle image processing. *eLife* **7** (2018).
11. S. H. Scheres, S. Chen, Prevention of overfitting in cryo-EM structure determination. *Nat Methods* **9**, 853-854 (2012).
12. A. Kucukelbir, F. J. Sigworth, H. D. Tagare, Quantifying the local resolution of cryo-EM density maps. *Nature methods* **11**, 63 (2014).
13. E. F. Pettersen *et al.*, UCSF Chimera—a visualization system for exploratory research and analysis. *Journal of computational chemistry* **25**, 1605-1612 (2004).
14. P. Emsley, K. Cowtan, Coot: model-building tools for molecular graphics. *Acta Crystallographica Section D: Biological Crystallography* **60**, 2126-2132 (2004).
15. P. D. Adams *et al.*, PHENIX: a comprehensive Python-based system for macromolecular structure solution. *Acta Crystallographica Section D: Biological Crystallography* **66**, 213-221 (2010).
16. V. B. Chen *et al.*, MolProbity: all-atom structure validation for

macromolecular crystallography. *Acta Crystallographica Section D: Biological Crystallography* **66**, 12-21 (2010).

17. N. Collaborative Computational Project, The CCP4 suite: programs for protein crystallography. *Acta Crystallogr D Biol Crystallogr* **50**, 760-763 (1994).

Supplementary Figures

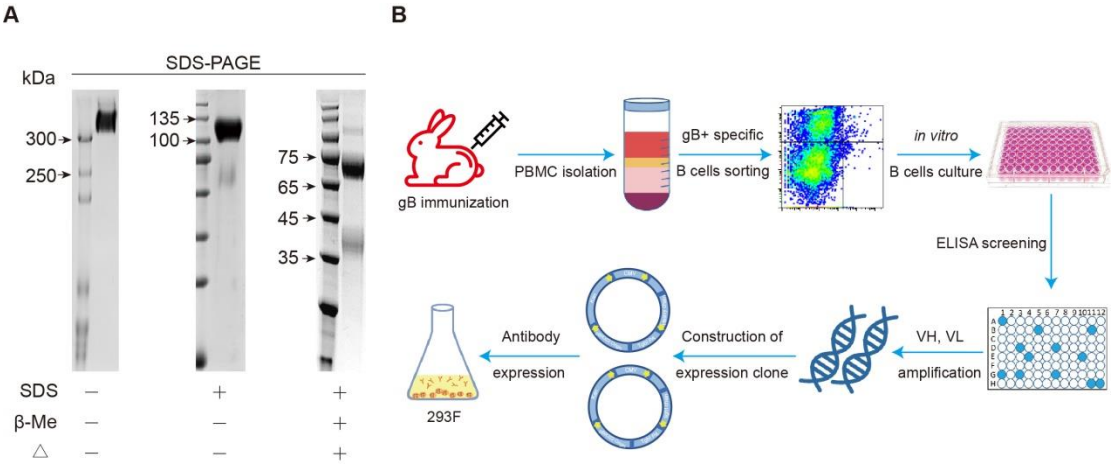

Figure S1. Characteristics of the recombinant gB ect-domain and the screening strategy for gB-specific antibodies

(A) Characteristics of recombinant gB ect-domain (ect-gB) expressed by 293F cells using SDS-PAGE. Left lane: ect-gB was treated under non-reducing conditions; middle lane: ect-gB was treated only with 0.1% SDS; right lane: ect-gB was treated under reducing conditions. Δ denotes heating at 100 °C for 5 min. Two bands with molecular weights of ~ 70 kDa and ~ 40 kDa were observed in the reducing SDS-PAGE.

(B) Workflow of antibody isolation from antiserum collected from gB-immunized rabbits. Briefly, the rabbit was immunized with purified gB protein. FACS was used to sort the gB-specific B cells from the PBMCs of immunized rabbits. The sorted B cells were cultured *in vitro*, and the medium was measured for its reactivity against gB by ELISA. Then, the variable fragments of the paired heavy (VH) and light (VL) chains were amplified using the positive B cells, and the recombinant plasmids were reconstructed. The plasmids were transfected into 293F cells for antibody expression.

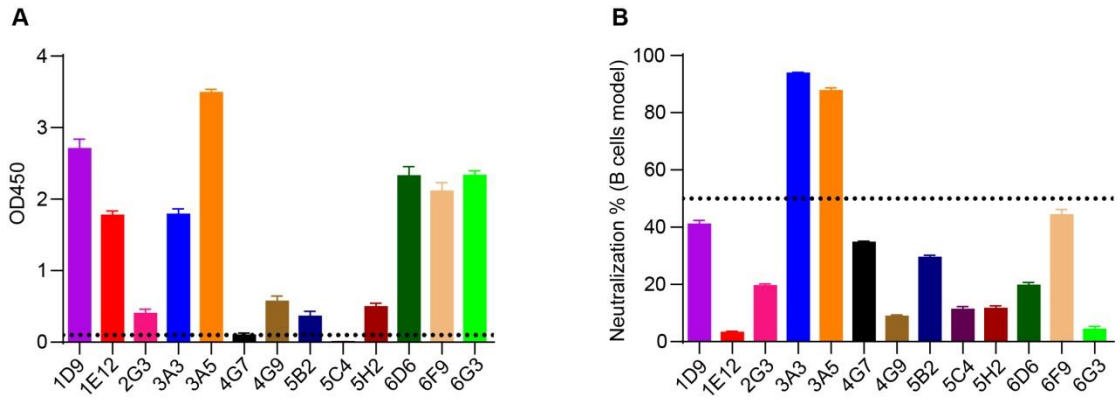

Figure S2. Binding and neutralizing abilities of a panel of monoclonal antibodies raised by ect-gB.

(A) Binding activities of mAbs detected by gB-based ELISA. The cutoff value was set as OD450=0.1.

(B) Neutralizing abilities of mAbs evaluated by a B cell (Akata cell) infection model. The cutoff value was set as neutralization%=50%.

Data are shown as the mean of two independent replicates ± SEM

A

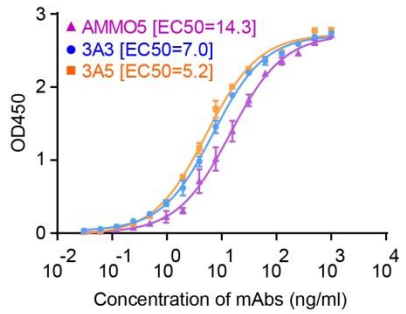

B

Fabs	Binding Kinetics of gB:Fab Complex		
	Ka (10^5/MS)	Kd (10^{-4}/S)	KD (nM)
3A3Fab	1.23±0.03	4.28±0.22	3.49±0.11
3A5Fab	14.15±1.05	54.80±4.40	3.93±0.61
AMMO5Fab	1.18±0.35	25.25±8.45	21.15±0.95

C

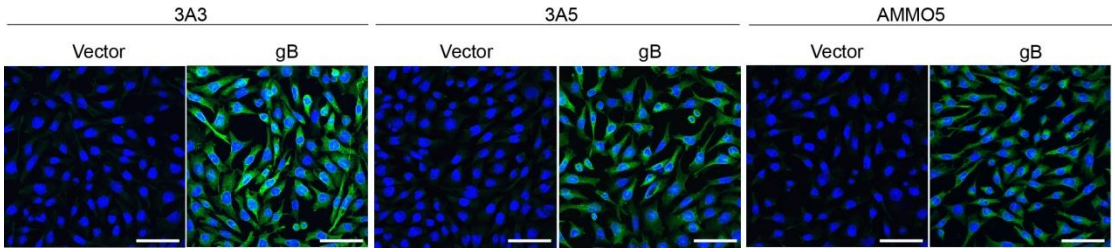

Figure S3. Evaluation of the binding and neutralizing abilities of 3A3 and 3A5.

(A) The binding activities of the three mAbs of 3A3, 3A5 and AMMO5 to gB were tested by ELISA, and the EC_{50} values were calculated by sigmoid trend fitting. Curves for 3A3, 3A5, and AMMO5 were colored blue, yellow and purple, respectively. Data are shown as the mean of two independent replicates ± SEM.

(B) The affinity constants of the interaction between gB coupled to the chip and the Fabs of 3A3, 3A5 or AMMO5 were measured by SPR in Biacore8000. The values are shown as the mean of two independent replicates ± SD.

(C) The binding of 3A3, 3A5, and AMMO5 to endogenously-expressed gB in COS7 fibroblast cells. Cells were stained with mAbs of 3A3, 3A5 and AMMO5, respectively, followed by goat anti-rabbit IgG AlexaFluor 488 or goat anti-human IgG AlexaFluor 488. A scale bar of 50 μm is shown.

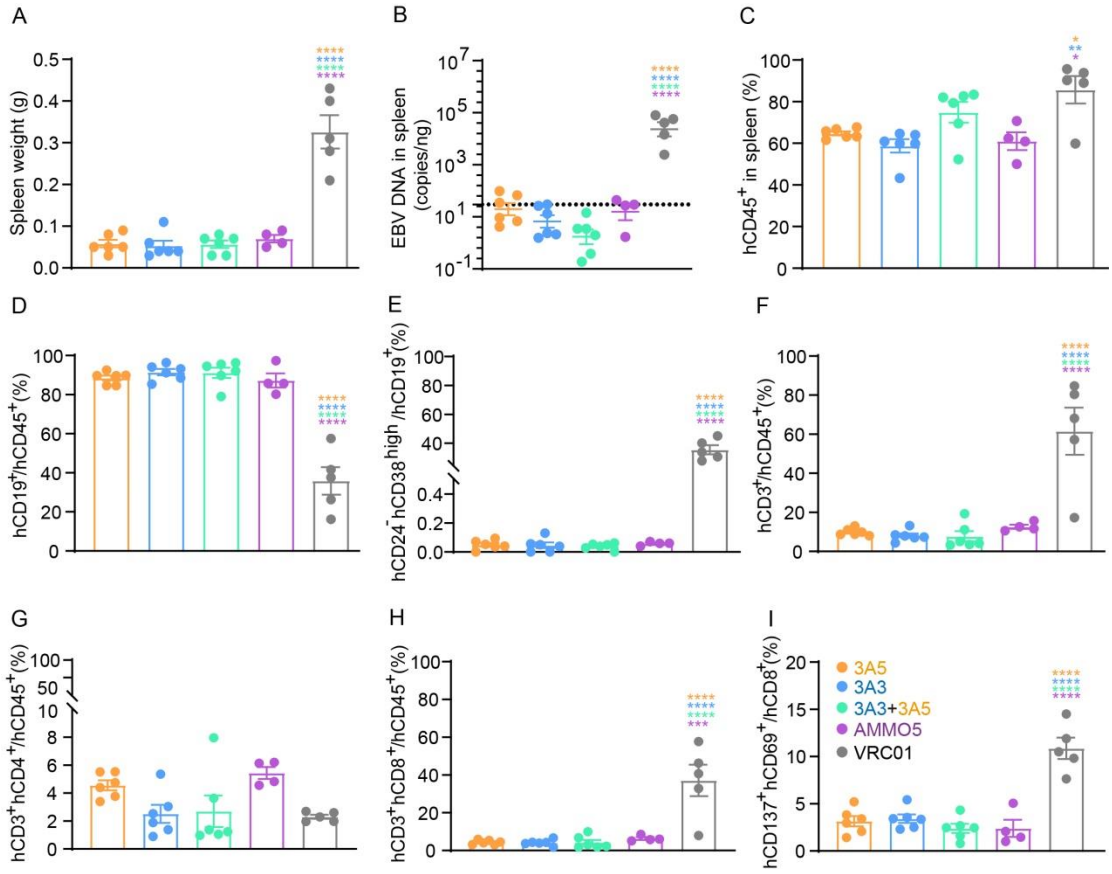

Figure S4. 3A3 and 3A5 conferred protection to humanized mice from EBV-induced LPD.

(A and B) Spleen weight (A) and EBV DNA copies in the spleens (B) were quantified at the experimental endpoint of each mouse.

(C-I) The percent changes for hCD45$^+$ (C), hCD19$^+$ (D), hCD19$^+$CD24$^-$CD38^{high} (E), hCD3$^+$ (F), hCD4$^+$ (G), hCD8$^+$ (H) and hCD8$^+$CD137$^+$CD69$^+$ (I) cells in the spleen over the experimental period. These data were collected and analyzed at the experimental endpoint of each mouse. Data points represent individual mice, and the mean error bars are shown as SE. For the AMMO5 group, two mice naturally died, and only four data points were collected. For the VRC01 group, one mouse naturally died, and five data points from five mice were collected. Among the five mice, four mice were euthanized because of >20% bodyweight loss, and only one survived to the experimental endpoint.

Data schematics for 3A3, 3A5, 3A3+3A5, AMMO5, and VRC01 were colored blue, yellow, green, purple, and black.

Statistical analyses were performed using one-way ANOVA. The color of the asterisks

534 (*$P \leq 0.0332$, **$P \leq 0.0021$, ****$P \leq 0.0001$) denotes the group with which there is a
535 significant difference from the VCR01-treated group, determined by a Sidak multiple
536 comparisons test.

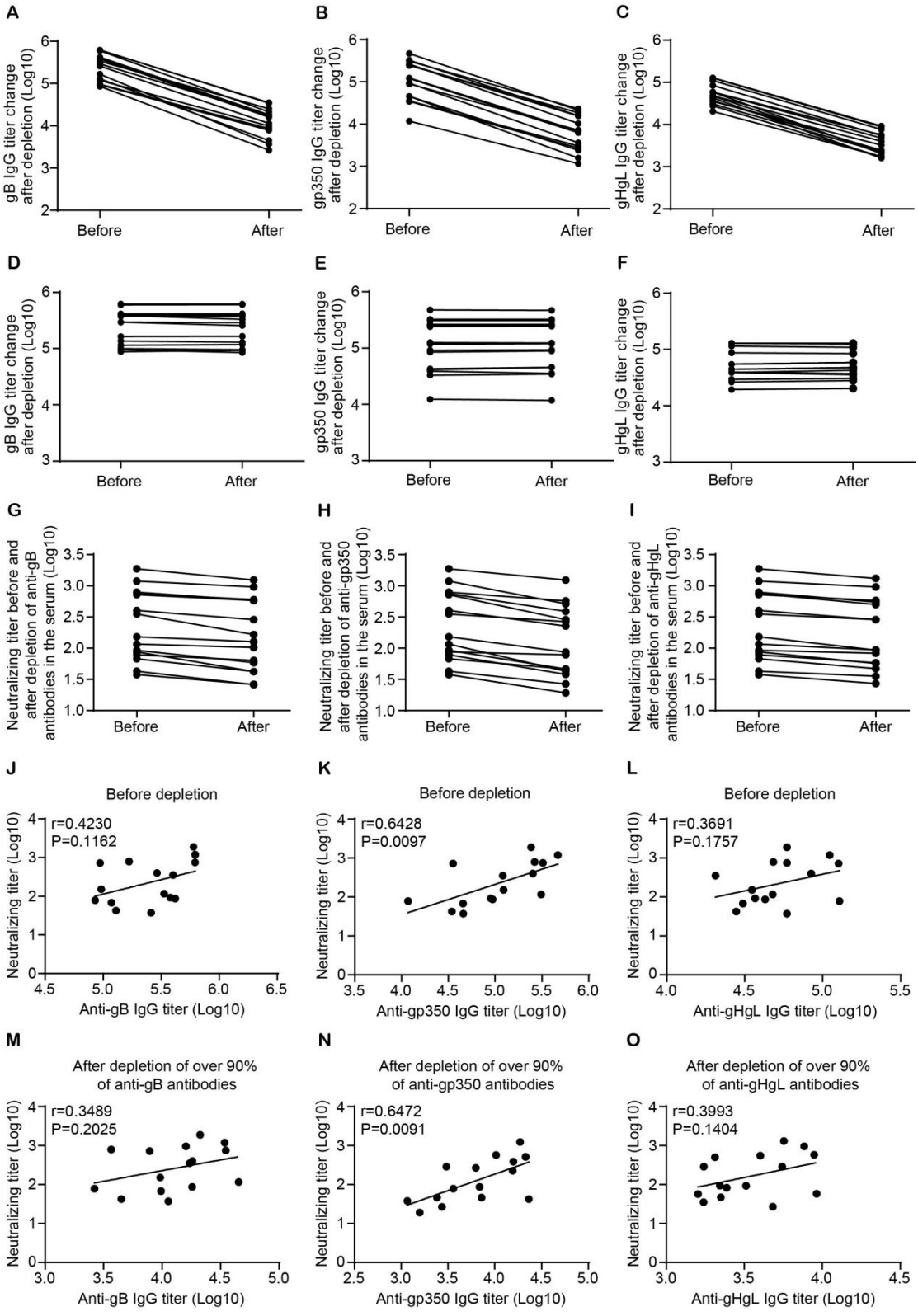

Figure S5. Evaluation of total IgG antibody titers against gB, gHgL, and gp350 in human sera and neutralizing titers using the B cell infection model.

(A-C) The serum IgG titers against gB (A), gp350 (B), and gHgL (C) before and after 15 rounds of depletion with 293T cells overexpressing gB, gp350, and gHgL,

542 respectively. (D-F) The serum IgG titers against gB (D), gp350 (E), and gHgL (F)
543 before and after the mock depletion assays using 293T cells transfected with the
544 empty vector. (G-H) The neutralizing titers of each serum before and after specific
545 depletion of over 90% of anti-gB (G), gp350 (H), and gHgL (I) antibodies,
546 respectively. The neutralizing titers before and after depletion were measured by the B
547 cell infection model. (J-O) The correlations between IgG titers against each
548 glycoprotein indicated and the neutralizing titers before (J-L) and after (M-O) the
549 specific antibody depletion. The correlation coefficients (r) between the IgG titers and
550 neutralizing titers were determined by the Pearson correlation coefficient. *P* values
551 from the two-tailed significance tests smaller than 0.05 are statistically significant.
552

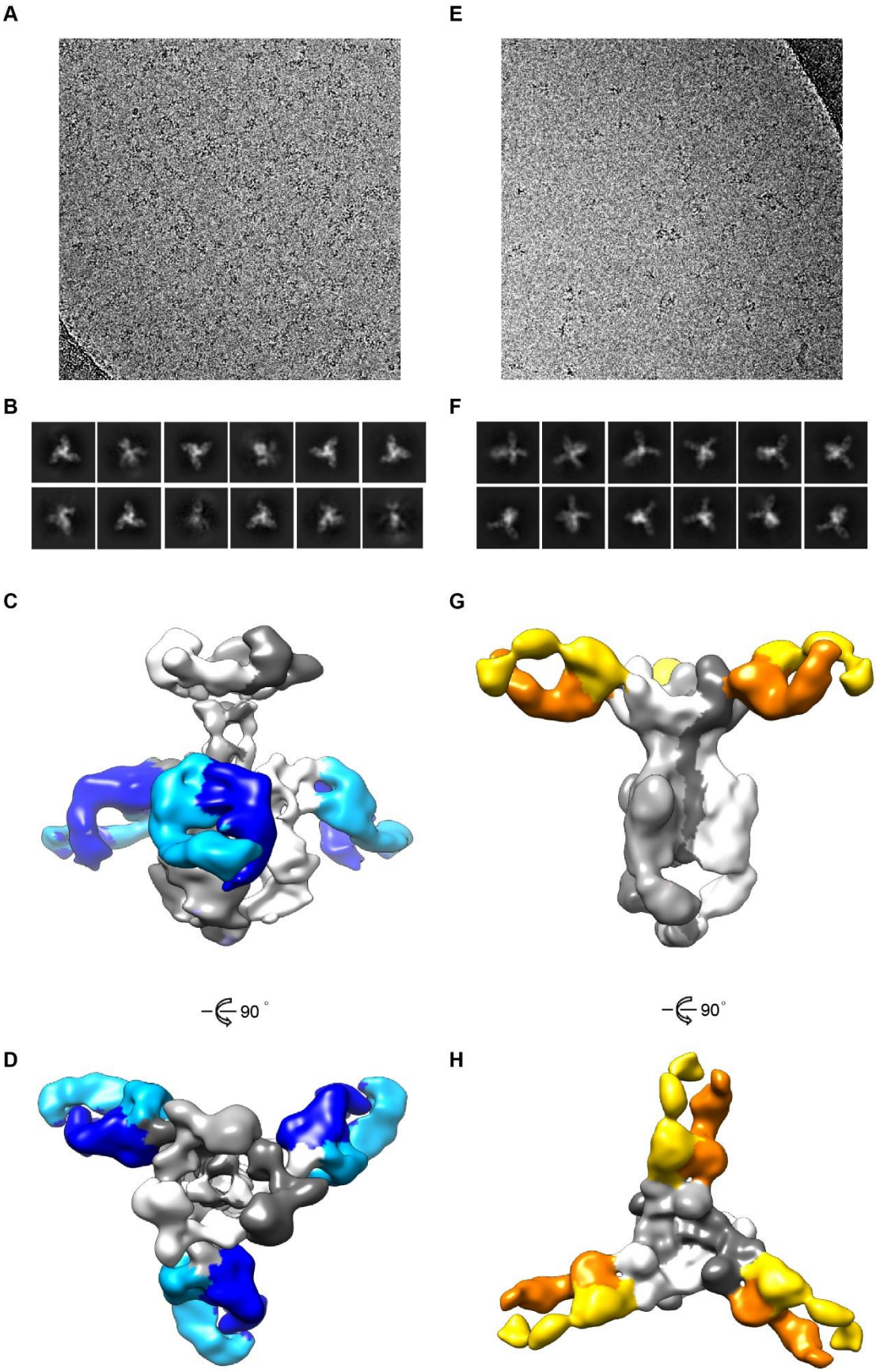

Figure S6. Cryo-EM reconstructions of gB:3A3Fab and gB:3A5Fab.

(A and E) Motion corrected micrographs of gB:3A3Fab (A) and gB:3A5Fab (E)

complexes, scale bar=50 nm.

(B and F) Representative 2D class averages of gB:3A3Fab (B) and gB:3A5Fab (F) were shown.

(C and D) The density map of gB:3A3Fab was shown in the side view (C) and top view (D). The gB trimer, the heavy chain, and the light chain of 3A3Fab were colored gray, blue, and cyan, respectively.

(G and H) The density map of gB:3A5Fab was shown in the side view (G) and top view (H). The heavy chain and light chain of 3A5Fab were colored orange and yellow, respectively.

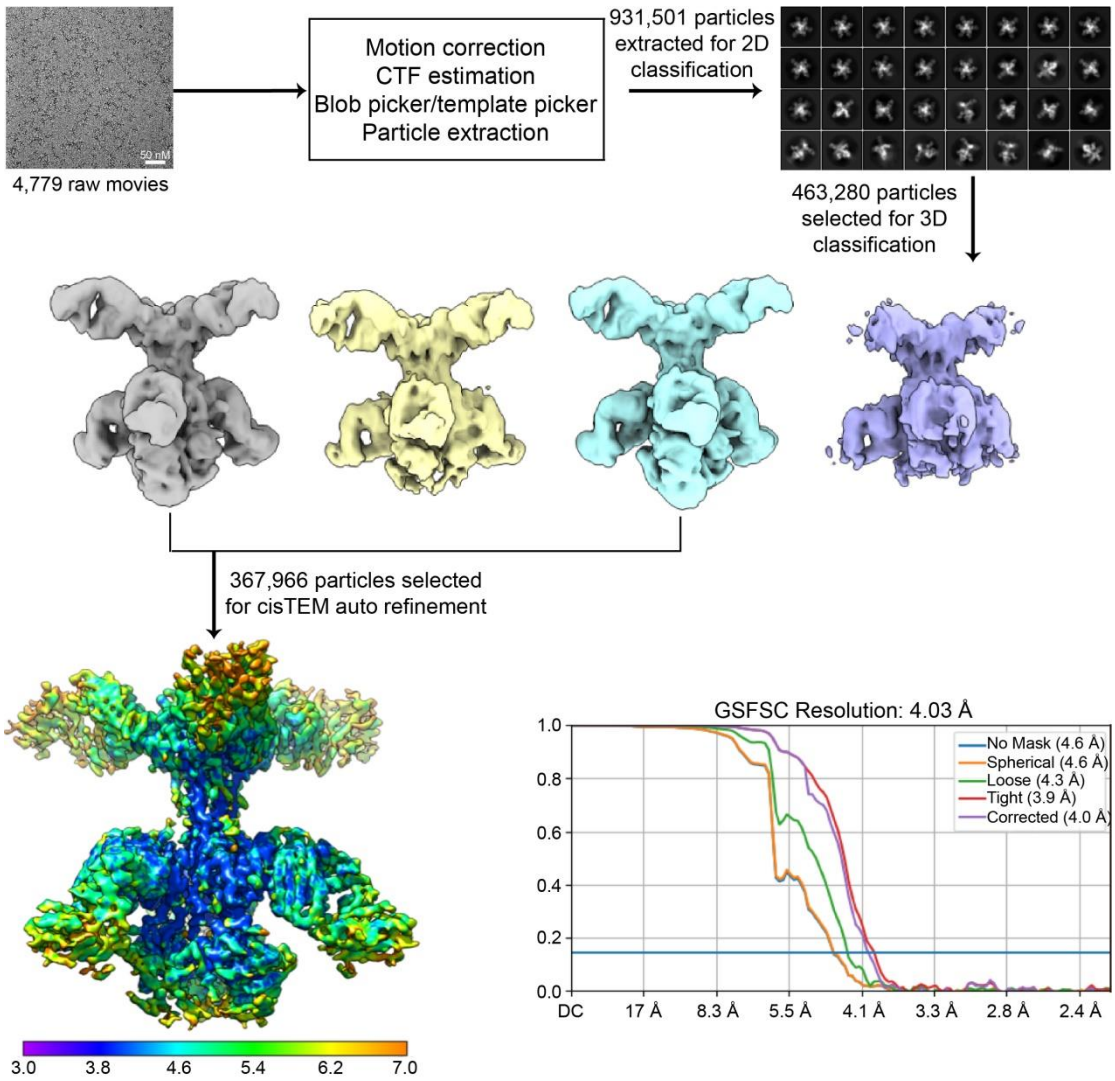

565

566 **Figure S7. Cryo-EM reconstruction of gB:3A3Fab:3A5Fab.**

567 Cryo-EM image processing flowchart for the immune complex of

568 gB:3A3Fab:3A5Fab. Representative results of the cryo-EM micrograph, 2D

569 classification, 3D classification, auto refinement, local resolution map, and FSC

570 curves are shown. Scale bar: 50nm.

571

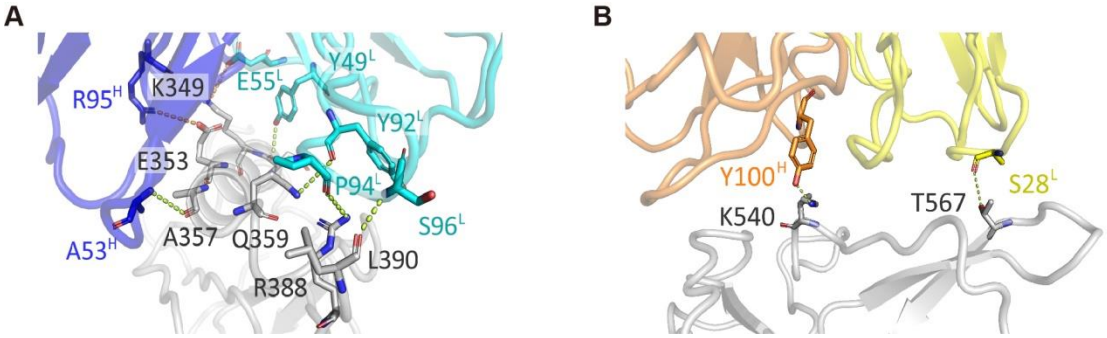

Figure S8. The detailed interaction at the interface of gB and 3A3 or 3A5.

(A) The residues involved in the 3A3 interactions were mapped on the gB surface including K349, E353, E356, A357, Q359, D360, R388, and L390. The key residues localized at the VH and VL chains of 3A3 are labeled, including $Y49^{L}$, $E55^{L}$, $Y92^{L}$, $P94^{L}$, $S96^{L}$, $A53^{H}$ and $R95^{H}$.

(B) The key residues involved in the 3A5 interactions were mapped on the gB surface including K540 and T567. The key residues localized at the VH and VL chains of 3A5 are labeled including $S28^{L}$ and $Y100^{H}$. The involved residues are displayed as sticks.

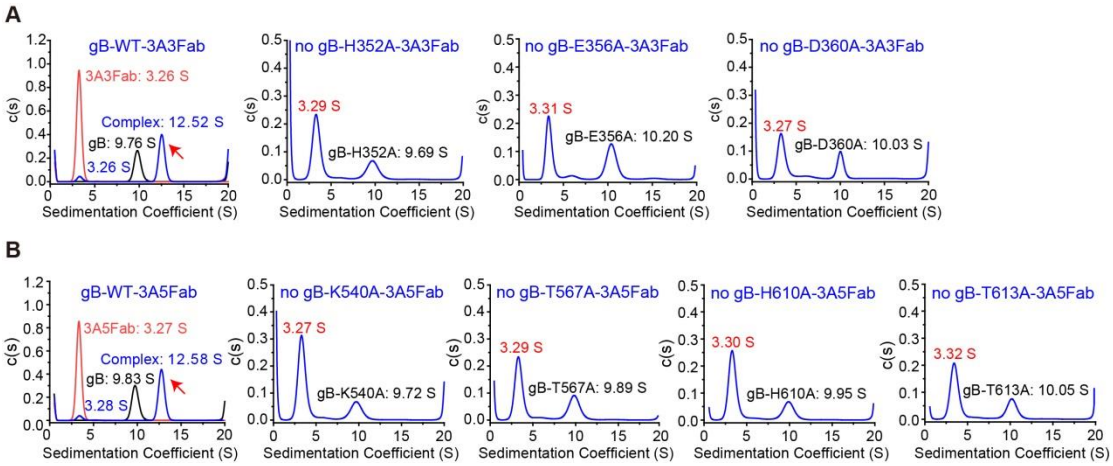

582

583 **Figure S9. Identification of the key residues referring to the interface of 3A3 or**

584 **3A5 and gB.**

585 Sedimentation velocities (SVs) were detected for the interaction of mAbs 3A3 (A)

586 and 3A5 (B) with mutant and wild-type gB. The c(s) profiles of 3A3Fab and 3A5Fab,

587 gB and the mutants, and the gB-Fab mixtures were denoted as red, black, and blue.

588

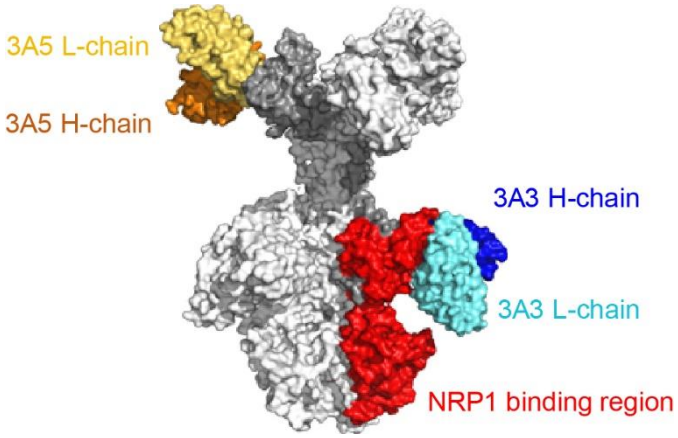

589

590 **Fig S10. Presentation of the binding region for NRP1, 3A3, and 3A5 on the gB**
591 **surface.** The binding regions of NRP1, 3A3 and 3A5 were colored red, blue, and
592 yellow, respectively.

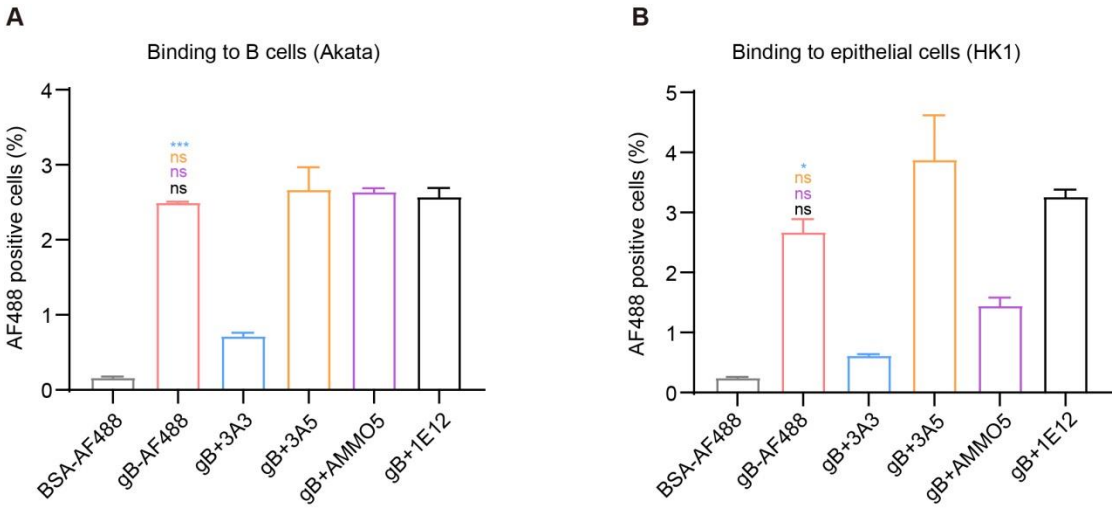

Figure S11. The blocking potential of different antibodies against the binding of gB to Akata cells (A) and HK1 cells (B).

Blocking effectivity of gB binding to Akata cells (A) and HK1 cells (B), respectively, by gB-specific mAbs 3A3, 3A5, AMMO5 and 1E12. BSA-AF488 was used as a negative control. gB-AF488 was used as a positive control. The results were represented as mean ± SEM.

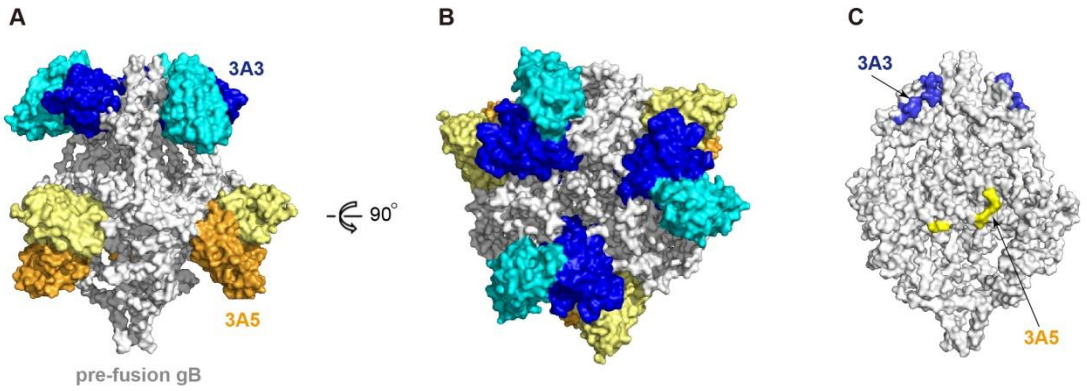

Figure S12. Presentation of the epitopes of 3A3 and 3A5 on the modeled pre-fusion gB surface.

The pre-gB was modeled using the homology template of HCMV pre-gB (PDB no: 7KDP). (A and B) The binding models of 3A3 and 3A5 to pre-fusion gB were shown (A, side view; B, top view). 3A3 in blue, 3A5 in yellow, and pre-gB in grey, respectively. (C) The epitopes recognized by 3A3 and 3A5 were indicated on the surface of pre-fusion gB. The epitopes recognized by 3A3 and 3A5 were labeled with blue and yellow, respectively.

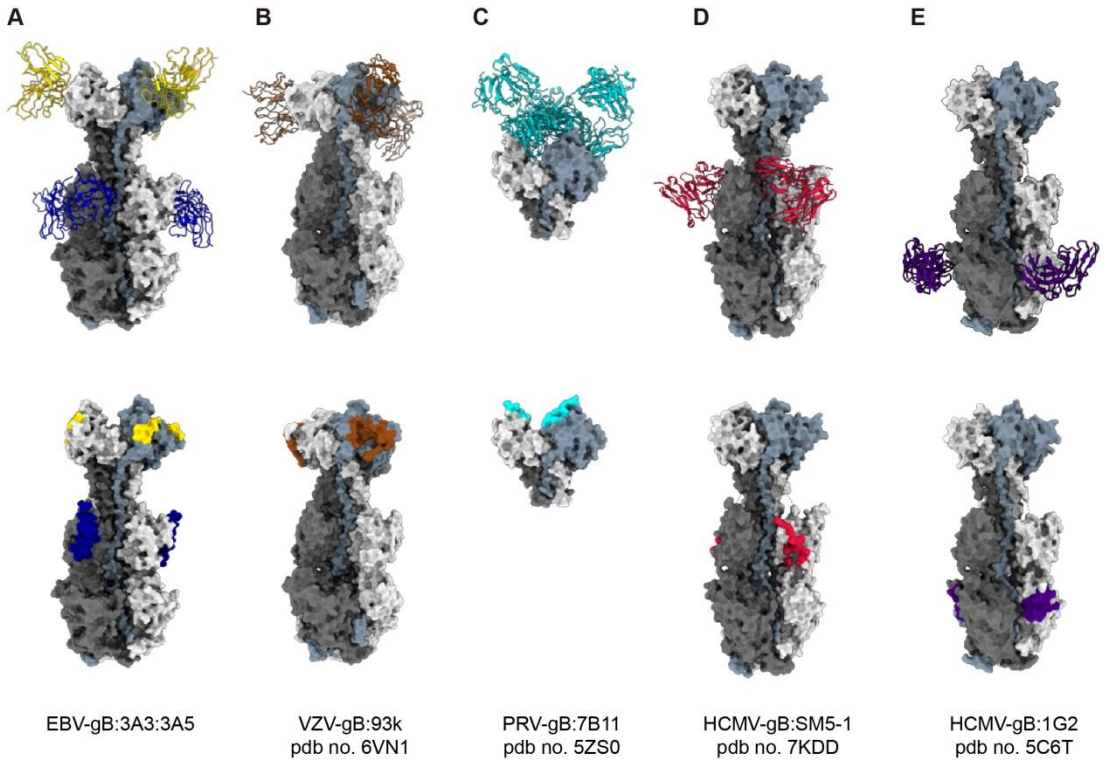

Figure S13. Comparison of the binding mode (upper panels) and binding sites (lower panels) of the representative anti-gB neutralizing antibodies (nAbs). 3A3/3A5 involved in this study (A), VZV-gB specific nAb 93k (B), PRV-gB specific nAb 7B11 (C), HCMV-gB specific nAbs SM5-1(D) and 1G2 (E) were shown. The gB timer was shown as surface representation and colored gray, dark gray and dim gray for each monomer. 3A3, 3A5, 93k, 7B11, SM5-1 and 1G2 were shown as sticks and colored yellow, blue, brown, cyan, red, and purple. The footprints of each nAb were shown in the lower panels and colored accordingly.

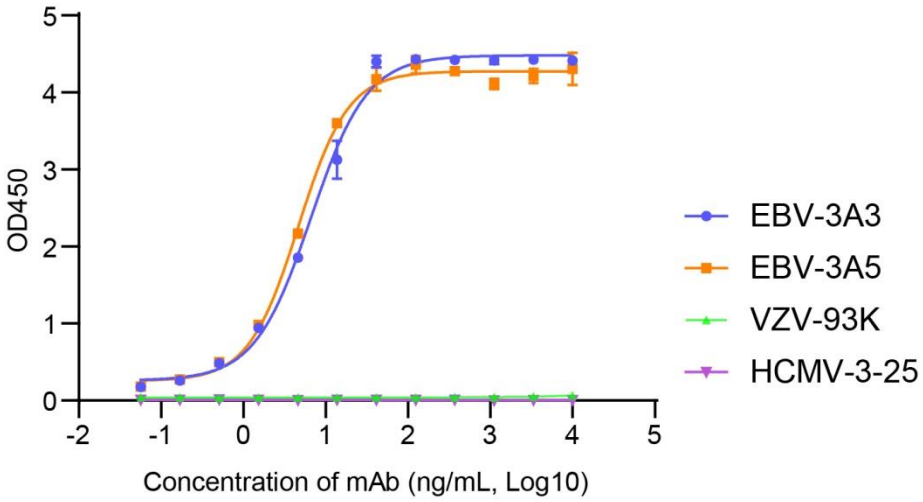

Fig S14. The binding activities of different nAbs against EBV, HSV, and HCMV to EBV-gB were evaluated by ELISA.

3A3 and 3A5 were involved in this study. VZV-specific nAb 93k recognizes D-IV of VZV-gB, and HCMV-specific nAb 3-25 recognizes D-II of HCMV-gB.

Supplementary Tables

Table S1. Variable region sequences of antibodies

No.	Antibodies	Chain	Homology	Gene sequence
1	3A3	VH	Orycun IGHV1S69*01 F	CAGTCAGTGAAGGAGTCCGGGGGTCGCCTGGTCACGCCTGGGACAC CCCTGACACTCACCTGCACAGTCTCTGGATTCTCCCTTAGTAGCTATG CAATGAGCTGGGTCCGCCAGGCTCCAGGGAAGGGGCTGGAATACAT CGGAGTCATTTATGCTAGTGGTAGCACATACTACGCGAGCTGGGCGA AAGGCCGATTCACCATCTCCAGAACCGCGACCACGGTGGATCTGAAA ATCACCAGTCCGACAACCGAGGACACGGCCACCTATTTCTGTGGCAG AGGGGTTTCTACTAACATGTGGGGCCCAGGCACCCTGGTCACCGTCT CTTCA
2	3A3	VK	Orycun IGKV1S34*01 F	GACCTCGTGATGACCCAGACTCCATCCTCCGTGTCTGCAGCTGTGGG AGGCACAGTCACCATCAAGTGCCAGGCCAGTCAGAGCCTTGGTGGT GGTTTAGCCTGGTATCAGCAGAAACCAGGGCAGCGTCCCAAGCTCCT GATCTATTCTGCATCCACTCTGGAATCTGGGGTCCCATCGCGGTTCAG AGGCAGTGGATCTGGGACAGAGTTCACTCTCACCATCAGCGACCTGG AGTGTGCCGATGCTGCCACTTACTACTGTCAAAGCGCTTATGGTCCTA CTAGTAATGGTCTTTTTAATGCTTTCGGCGGAGGGACCAAGGTGGTCA TCAAA
3	3A5	VH	Orycun IGHV1S69*01 F	CAGTCGGTGAAGGAGTCCGGGGGTCGCCTGGTCACGCCTGGGACAC CCCTGACACTCACCTGCACAGTCTCTGGATTCTCCCTCAGTAGTTATG AAATGGGCTGGGTCCGCCAGGCTCCAGGGGAGGGGCTGGAATGGAT CGGAACCATTAGTACTGGTGGTAGTTCATACTACGCGAGCTGGGCAA AAGGCCGATTCACCATCTCTAGAACCTCGACCACGGTGGATCTGAAA

				ATGACCAGTCTGACAACCGCGGACACGGCCACCTATTTCTGTGCCAG AGGTTATGGTGGTTATGGCATTGGTGCAGGCTACTTTAACATCTGGGG CCCAGGCACCCTGGTCACCGTCTCTTCA
4	3A5	VK	Orycun IGKV1S3*02 F	GCCCTCGTGATGACCCAGACTCCATCCTCCGTGTCTGAACCTGTGGG AGGCACAGTCACCATCAAGTGCCAGGCCAGTCAGAGCATTAGTAGTT ACTTAGCCTGGTATCAGCGGAAACCAGGGCAGCGTCCCAAACTCCTG ATCTATGGTACATCCACTCTGGCATCTGGGGTCCCATCGCGGTTTATTG GCAGTGGATCTGGGACAGACTACACTCTCACCATCAGCGACCTGGAA TGTGACGATGCTGCCACTTACTACTGTCAACAGGGTTTTAGTACTAGT AATGTTTATAATTCTTTCGGCGGAGGGACCAAGGTGGACATCAAA
5	1E12	VH		CAGTCAGTGAAGGAGTCCGGGGGTCGCCTGGTCACGCCTGGGACAC CCCTGACACTCACCTGCACCGTCTCTGGAATCGACCTCAGTACCTATG TAATGACTTGGGTCCGCCAGGCTCCAGGGAAGGGGCTGGAATGCATC GGAATCATTGGTTATGGTGGTAGCACATACTACGCGAGCTGGGCGAC AGGCCGATTCACCATCTCCAAAACCTCGACCACGGTGGATCTGAGAA TGACCAGTCTGACAACCGAGGACACGGCCACCTATTTCTGTGCCAGA GGTGTTAGTAGTAATCTTTATAGGGGAATGAATTTGTGGGGCCAAGGC ACCCTGGTCACCGTCTCTTCA
6	1E12	VK		GCCCTCGTGATGACCCAGACTCCATCTCCCGTGTCTGCAGCTGTGGG AGGCACAGTCAGCATCAGTTGCCAGTCCAGTCCGAGTGTTTATAGTA ATTACTTATCCTGGTATCAGCAGAAACCAGGGCAGCCTCCCAAGCTC CTGATCTACGAAACATCCAAACTGGAATCTGGGGTCCCATCGCGGTT CAGCGGCAGTGGATCTGGGACACAGTTCACTCTCACCATCAGCGGCG TGCAATGTGACGATGCTGCCACTTACTACTGTGCAGGCGGTTATAGTG GTATTAGTGATACGTTTGCTTTCGGCGGAGGGACCAAGGTGGACATC AAA

Table S2. Summary of blocking activity of anti-gB mAbs 3A3, 3A5, 3A3+3A5, 1E12, and the anti-HA mAb 2G9 in the sera from 15 healthy donors and 15 patients with NPC measured by ELISAs with immobilized recombinant gB and flow cytometry assays with membrane-bound gB expressed by 293T cells.

	Healthy donors (15 sera)					**Patients with NPC (15 sera)**				
	3A3	3A5	3A3+3A5	1E12	2G9	3A3	3A5	3A3+3A5	1E12	2G9
ELISA with recombinant gB	34.63±2.77	32.17±2.84	71.14±2.74	9.55±0.93	3.67±0.59	41.33±2.32	44.59±2.87	74.50±2.51	9.53±1.05	3.72±0.41
Flow Cytometry with membrane-bound gB	36.64±5.47	30.13±3.78	73.40±2.93	9.76±1.77	4.47±0.79	33.89±4.38	31.27±3.87	67.04±2.65	9.17±1.70	3.23±0.51
***P* value**	0.75	0.67	0.58	0.92	0.43	0.15	0.01	0.05	0.86	0.46

The results of ELISAs and flow cytometry assays that used the same sera from 15 healthy donors and 15 patients with NPC are shown as mean ± SEM for each experimental group. *P* values from the unpaired Welch's *t*-tests of whether the results differ between ELISAs and flow cytometry assays are indicated.

Table S3. CryoEM data collection and atomic model refinement statistics

	gB:3A3Fab	gB:3A5Fab	gB:3A3 Fab:3A5 Fab
Data collection and processing			
Magnification	93,000	93,000	23,000
Voltage (kV)	300	300	300
Electron exposure (e-/A^2)	30	30	56
Defocus range (μm)	1.2-3.5	1.2-3.5	0.8-2.5
Pixel size (Å)	1.12	1.12	1.10
Symmetry imposed	C3	C3	C3
Final particle images (no.)	9,270	18,826	367,966
Map resolution (Å)	7.1	9.0	3.9
FSC threshold	0.143	0.143	0.143
Map sharpening B factor ($Å^2$)	-90	-90	-200
Validation			
MolProbity score	/	/	2.21
Clashscore	/	/	10.87
Poor rotamers (%)	/	/	0.35
Ramachandran plot			
Favored (%)	/	/	85.24
Allowed (%)	/	/	14.66
Disallowed (%)	/	/	0.10

Table S4. Primers used in this study

No.	Instructions for primers	Oligonucleotides
1	Forward primer for fusion loop (WY) mutation of wild-type gB	5’-TCATCTACAATGGCCACCGCGCGGACTCCGTGACCAACCGGCACGA-3’
2	Reverse primer for fusion loop (WY) mutation of wild-type gB	5’-TCCGCGCGGTGGCCATTGTAGATGAGAATGTTGGTCACTATCTTGGT-3’
3	Forward primer for fusion loop (WLIW) mutation of wild-type gB	5’-GCCCCCGGGCGGGTGGAGGCGACTTACAGAACAAGAACTACCGTCA-3’
4	Reverse primer for fusion loop (WLIW) mutation of wild-type gB	5’-TAAGTCGCCTCCACCCGCCCGGGGGCGTCATAGAGCTCCGTCTGGC-3’
3	Forward primer for gB-E345A	5’-ATCGAAGCCCAGGTGAACAAGACCATGCAT-3’
4	Reverse primer for gB-E345A	5’-GTTCACCTGGGCTTCGATGCACTTGAAG-3’
5	Forward primer for gB-N348A	5’-AGAGCAGGTGGCCAAGACCATGCATGAAAA-3’
6	Reverse primer for gB-N348A	5’-GCATGGTCTTGGCCACCTGCTCTTCGATGCAC-3’
7	Forward primer for gB-K349A	5’-GTGAACGCCACCATGCATGAAAAGTACGAG-3’
8	Reverse primer for gB-K349A	5’-CATGGTGGCGTTCACCTGCTCTTCGATGCACTTG-3’
9	Forward primer for gB-H352A	5’-ACCATGGCCGAAAAGTACGAGGCCGTC-3’

10	Reverse primer for gB-H352A	5’-ACTTTTCGGCCATGGTCTTGTTCACCTGC-3’
11	Forward primer for gB-E353A	5’-ACCATGCATGCCAAGTACGAGGCCGTC-3’
12	Reverse primer for gB-E353A	5’-CGTACTTGGCATGCATGGTCTTGTTCACCTG-3’
13	Forward primer for gB-E356A	5’-AAAGTACGCCGCCGTCCAGGATCGTTACA-3’
14	Reverse primer for gB-E356A	5’-ACGGCGGCGTACTTTTCATGCATGGTCTTG-3’
15	Forward primer for gB-Q359A	5’-CCGTCGCCGATCGTTACACGAAGGGCCAG-3’
16	Reverse primer for gB-Q359A	5’-TAACGATCGGCGACGGCCTCGTACTTTTCA-3’
17	Forward primer for gB-D360A	5’-TCCAGGCCCGTTACACGAAGGGCCAGGAA-3’
18	Reverse primer for gB-D360A	5’-TGTAACGGGCCTGGACGGCCTCGTACTTT-3’
19	Forward primer for gB-R388A	5’-TCTGACCCCGGCCTCGTTGGCCACCGTCAAG-3’
20	Reverse primer for gB-R388A	5’-TGGCCAACGAGGCCGGGGTCAGAGGTAGCCAA-3’
21	Forward primer for gB-L390A	5’-CCCGCGCTCGGCCGCCACCGTCAAGAACCTGA-3’
22	Reverse primer for gB-L390A	5’-TGACGGTGGCGGCCGAGCGCGGGGTCAGAGGT-3’
23	Forward primer for gB-R539A	5’-GTCACCCTGGCCAAGAGCATGAGGGTCCCC-3’
24	Reverse primer for gB-R539A	5’-TCATGCTCTTGGCCAGGGTGACGGTGGCCT-3’
25	Forward primer for gB-K540A	5’-ACCCTGCGCGCCAGCATGAGGGTCCCCGGC-3’
26	Reverse primer for gB-K540A	5’-CTCATGCTGGCGCGCAGGGTGACGGTGGCC-3’

27	Forward primer for gB-S558A	5’-CCCCCTGGTGGCCTTCAGCTTTATCAACGA-3’
28	Reverse primer for gB-S558A	5’-TAAAGCTGAAGGCCACCAGGGGGCGCGAGTAG-3’
29	Forward primer for gB-T565A	5’-TATCAACGACGCCAAGACCTACGAGGGACA-3’
30	Reverse primer for gB-T565A	5’-AGGTCTTGGCGTCGTTGATAAAGCTGAAGG-3’
31	Forward primer for gB-K566A	5’-CAACGACACCGCCACCTACGAGGGACAGCT-3’
32	Reverse primer for gB-K566A	5’-CGTAGGTGGCGGTGTCGTTGATAAAGCTGA-3’
33	Forward primer for gB-T567A	5’-CGACACCAAGGCCTACGAGGGACAGCTGGG-3’
34	Reverse primer for gB-T567A	5’-CCTCGTAGGCCTTGGTGTCGTTGATAAAGC-3’
35	Forward primer for gB-H610A	5’-CGACTACCACGCCTTTAAAACCATCGAGCT-3’
36	Reverse primer for gB-H610A	5’-TTTTAAAGGCGTGGTAGTCGTTGTAGACGT-3’
37	Forward primer for gB-F611A	5’-CTACCACCACGCCAAAACCATCGAGCTGGA-3’
38	Reverse primer for gB-F611A	5’-TGGTTTTGGCGTGGTGGTAGTCGTTGTAGA-3’
39	Forward primer for gB-K612A	5’-CCACCACTTTGCCACCATCGAGCTGGACGG-3’
40	Reverse primer for gB-K612A	5’-CGATGGTGGCAAAGTGGTGGTAGTCGTTGT-3’
41	Forward primer for gB-T613A	5’-CCACTTTAAAGCCATCGAGCTGGACGGCAT-3’
42	Reverse primer for gB-T613A	5’-GCTCGATGGCTTTAAAGTGGTGGTAGTCGT-3’